Infectious subgenomic amplicon strategies for Japanese encephalitis and West Nile viruses

Prince Pal Singh[1,2], Nguyen Phuong Khanh Le[1], Uladzimir Karniychuk[1,*]

Number of words with references: 5,237

[1]Department of Veterinary Biosciences, College of Veterinary Medicine, The Ohio State University, Columbus, OH, USA

[2]School of Public Health, University of Saskatchewan, Saskatoon, Canada

***Correspondence:** Uladzimir Karniychuk

Department of Veterinary Biosciences, College of Veterinary Medicine, The Ohio State University, Columbus, OH, USA

karniychuk.1@osu.edu

ABSTRACT

Classical methods for constructing infectious cDNA clones of flaviviruses are often hindered by instability, toxicity, and laborious procedures. The Infectious-Subgenomic-Amplicons (ISA) method represents a significant advancement by utilizing overlapping DNA fragments representing viral genomic sequence and in-cell recombination to bypass bacterial plasmid assembly, simplifying the process. However, the ISA method has limitations due to the toxicity of some ISA DNA fragments in bacteria during synthetic production. We validated modified ISA strategies for producing toxic ISA Japanese encephalitis virus (JEV) and West Nile virus (WNV) fragments synthetically. Three approaches were explored including subdividing toxic DNA fragments into two sub-fragments for synthetic clonal production, using a low-copy bacterial plasmid, and subdividing the toxic DNA fragments into four short overlapping sub-fragments, each up to 1.8 kb. The latter novel approach in ISA applications enabled the synthesis of entirely bacteria-free ISA fragments and synthetic WNV. Our results demonstrate that subdividing toxic fragments into sub-fragments smaller than 1.8 kb for synthesis is the efficient strategy, circumventing the need for bacterial plasmids and ensuring rapid production of synthetic flaviviruses. This method also shortens the production timeline. In conclusion, the modified ISA strategies validated in this study provide a robust and efficient approach for producing entirely synthetic JEV and WNV. These advancements have significant implications for virology, enabling rapid research responses during outbreaks of emerging flaviviruses by facilitating the quick generation of new virus variants.

Flavivirus, Japanese encephalitis virus, West Nile virus, dengue virus, infectious subgenomic amplicons, ZAP, reverse genetics, infectious clones, recombinant virus

INTRODUCTION

Flaviviruses are single-stranded RNA viruses transmitted mainly by arthropods, as well as sexually and transplacentally. The genus Flavivirus (family *Flaviviridae*) comprises viruses which cause human disease, including dengue virus (DENV), Japanese encephalitis virus (JEV), and West Nile virus (WNV). These flaviviruses infect millions of people each year, causing symptoms from mild fevers to fatal hemorrhagic and neurological diseases [1]. The rising number of global flavivirus infections, frequent outbreaks, and expanding geographical range pose significant public health concerns [1]. Flaviviruses also pose constant threats to livestock industries [2]. Despite these threats, there are no approved human vaccines for certain flaviviruses, such as Zika virus and WNV. Moreover, no licensed antivirals exist against flaviviruses.

There are four DENV serotypes, causing illnesses ranging from mild dengue fever to severe, life-threatening dengue. Dengue virus is the major cause of hospitalization and death in children in Southeast Asian countries. Annually, DENV results in approximately 390 million infections, 100 million clinically apparent cases, and 500,000 severe cases, with at least 2.5 billion people at risk [1,3]. Over the past 70 years, infection rates have steadily increased, making DENV the most prevalent arthropod-borne viral disease worldwide. By comparison, only sporadic DENV epidemics were documented before the Second World War [1,4]. Between 2010 and 2022, more than 33,000 locally acquired dengue cases have been reported in the USA. Since 2014, there have been fewer than 1,000 cases per year, but 2022 was the first time in a decade that cases reached four digits. In 2023, Florida officials issued a warning about dengue as the cases continued to increase.

Japanese encephalitis virus causes encephalitis in humans in the Asia-Pacific region [5], with 68,000 annual cases and 15,000 deaths [6]. JEV epidemics were originally described in Japan in the 19th century, and the virus was first recovered in 1935 from an infected human in Tokyo [1]. The enzootic cycle of JEV is between water birds and *Culex* mosquitoes, with pigs also serving as an amplifying host [1]. Humans are considered incidental dead-end hosts and generally do not produce viremia sufficient to infect mosquitoes. Though many human infections are asymptomatic, around 20-30% of clinical infections are fatal, and 30-50% of the survivors develop life-long neurological sequelae [5]. Human transplacental and fetal JEV infections are also reported [7]. The geographic range of emerging JEV keeps expanding from the South of Russia to Australia, Japan, Eastern China, India, and South-East Asia. Also, severe travel-related cases are reported around the globe [8]. There is a concern that JEV can be introduced into North America given a large population of susceptible avian species and amplifying hosts—pigs, wild boars; susceptible *Culex* mosquitoes are also ubiquitous [9-11]. In addition to morbidity and mortality in humans, JEV causes economically significant clinical disease in pigs, mostly abortions and stillbirth [11,12]. Japanese encephalitis virus keeps expanding—the 2022 JEV outbreak in Australia with infections in swine herds, zoonotic transmission, and human deaths was caused by genotype IV which was not associated with outbreaks before [13].

West Nile virus (WNV) is classified by the National Institute of Allergy and Infectious Diseases as a "Category B Priority" pathogen, indicating its high threat level. West Nile virus cycles between *Culex* mosquitoes and birds, but it can also infect humans, horses, and other mammals. The virus is widespread, found in Africa, the Middle East, West Asia, Australia, the Americas, and Europe. The first major European outbreak occurred in Romania in 1996, with the largest in

93 2018 affecting 12 countries. In the U.S., WNV emerged in 1999, rapidly spreading and causing
94 significant morbidity and annual outbreaks, notably in 2002, 2003, and 2012 [1,14].
95 West Nile virus is neuroinvasive, leading to central nervous system damage, including
96 meningitis and encephalitis, which can be fatal or cause long-term disabilities such as a
97 poliomyelitis-like syndrome. The virus's spread has increased due to expanding mosquito
98 habitats and changing bird migration patterns caused by climate change. Currently, it is the most
99 common insect-borne zoonotic virus in the U.S., with no approved human vaccines or antivirals.
100 From 1999 to 2010, blood supply screening estimated 2 to 4 million total infections in the U.S.
101 [15]. In 2022, Centers for Disease Control and Prevention reported 1,126 cases and 93 deaths in
102 the U.S., and 2,406 cases and 1,599 neuroinvasive diseases in 2023, underscoring growing cases
103 and inadequate environmental controls.
104
105
106 Reverse genetics, defined as the generation of viruses entirely from complementary DNA
107 (cDNA) [16], has revolutionized virology research, including research of flaviviruses. This
108 powerful technique enables the experimental editing of viral genomes to investigate effects of
109 point mutations, host-pathogen interactions, virulence factors, mechanisms of immune evasion,
110 and the development of reporter viruses, vaccines, and antiviral testing [17,18]. The classical
111 method involves constructing an infectious DNA clone. This clone is typically a bacterial DNA
112 plasmid or two plasmids containing the entire cDNA of the viral genome and a suitable
113 promoter, such as the T7 promoter [17,19]. In this approach, viral RNA is obtained from
114 biological specimens, and a double-stranded cDNA copy of the RNA virus genome is generated
115 and incorporated into plasmids, which are then amplified in bacteria. After plasmid purification,

116 infectious viruses are produced either by direct transfection of permissive cells or by transfection
117 of genomic RNA obtained through *in vitro* transcription [17,19].
118
119 Despite advances in molecular techniques, classical methods for constructing infectious cDNA
120 clones are time-consuming, unpredictable, and labor-intensive and frequently associated with
121 undesirable mutations or unstable and toxic clones in bacteria [17,19]. Flavivirus infectious DNA
122 clones are particularly challenging due to the instability and toxicity of some viral sequences in
123 bacterial hosts [17-23]. To mitigate these difficulties, bacteria-free approaches have been
124 developed, including long PCR, circular polymerase extension reaction, Gibson assembly, and
125 Infectious-Subgenomic-Amplicons (ISA) [17].
126
127 The ISA method represents a significant advancement in reverse genetics for flaviviruses [24]. It
128 allows to bypass the problematic step of assembling and amplifying the full-length flavivirus
129 genome in bacterial plasmids and cells. Instead, the ISA process relies on in-cell recombination,
130 which simplifies and shortens the procedure where overlapping PCR-amplified ISA DNA
131 fragments, flanked with a pCMV promoter and HDR/SV40pA sequences, are directly transfected
132 into mammalian cells, insect cells, or *in vivo* in mice [17,25]. For example, in the most recent
133 study using the classical ISA the authors rescued DENV; in contrast cloning the full-length
134 DENV genome in bacteria failed due to toxicity [19].
135
136 While ISA is termed a "bacteria-free" approach, it is not completely free of bacteria and
137 associated toxicity issues. Specifically, to our knowledge all sixteen published studies utilizing
138 ISA for flavivirus rescue have used PCR amplification of fragments from pre-existing full-length

flavivirus DNA infectious clones, infected biological specimens, or synthetic overlapping DNA ISA fragments. These later synthetic DNA fragments, provided by commercial suppliers, are assembled, inserted into bacterial plasmids, and amplified in bacteria [19,24-38]. Although this approach avoids constructing unstable and toxic plasmids containing sequences of the entire viral genome, some synthetic ISA DNA fragments still may pose bacterial toxicity, slowing or halting their commercial production. Indeed, in several of these papers, along with commercially generated ISA DNA fragments, the authors PCR-amplified some ISA fragments directly from historically preexisting entire-genome-length flavivirus infectious DNA clones or from infected biological specimens to rescue yellow fever virus, DENV, and JEV [24,34]. While the reason for applying this mixed, not entirely synthetic reverse genetics approach was not explicitly explained in these publications, it is likely due to the toxicity of ISA DNA fragments preventing commercial generation of fragments for fully synthetic flaviviruses.

In our studies, we encountered similar technical difficulties with the toxicity of flavivirus ISA DNA fragments, which impeded commercial suppliers' ability to provide the required fragments. Given the importance of generating entirely synthetic flavivirus stocks for certain experimental objectives, in this study we applied and validated modified ISA strategies. These approaches allowed us to generate JEV and WNV using a completely synthetic method for toxic ISA flavivirus fragments.

162 **MATERIALS AND METHODS**

163 Wild-type and CCCH-type zinc finger antiviral protein (ZAP) knockout cells, *in silico*
164 permutation of the viral genome, ISA, DENV, JEV, and WNV stock generation and titration,
165 comparative ISA, mouse experiments, RT-qPCR, and statistics are described in supplemental
166 materials and methods.

167

168 **RESULTS**

169 **Classical Infectious-Subgenomic-Amplicons method for dengue virus**

170 As described before [19], transfection of three overlapping ISA DNA fragments generated via
171 *synthetic clonal genes* with medium copy number bacterial plasmids (**Table S1**) and
172 amplification in bacteria (**Fig 1**) consistently rescued infectious DENV in all five well replicates.
173 The virus induced a cytopathic effect (CPE) in all transfected wells at passages 0 and 1 (**Fig 2A**),
174 as well as in flasks during subsequent passaging and virus stock generation. Sanger sequencing
175 confirmed correct sequences in the DENV stock. The DENV stock produced in VERO-ZAP-KO
176 cells exhibited high infectious titers when titrated on both VERO-ZAP-WT and VERO-ZAP-KO
177 cells (**Fig 2B**), along with high viral RNA loads (**Fig 2C**) and E protein expression (**Fig 2D**).

178

179 Altogether, as in the previous study [19], we confirmed that classical ISA (**Fig 1**) with three
180 overlapping DNA fragments generated via *synthetic clonal genes* with bacterial plasmids is a
181 highly efficient and robust technique for type 2 DENV reverse genetics, enabling the rescue of
182 synthetic recombinant viruses. The properties of ISA-derived DENV have been extensively

183 characterized in prior research [19]; thus, we further focused on the more challenging ISA
184 strategies for JEV and WNV.
185

186 **Infectious-Subgenomic-Amplicons method to overcome bacterial toxicity caused by**
187 **Japanese encephalitis virus sequences**

188 In contrast to DENV, classical ISA failed to rescue the JEV SA14-2-14 strain. The JEV
189 Fragment I exhibited bacterial toxicity across three different medium and low copy bacterial
190 plasmids (**Table S1, Fig 3**). To overcome this, we divided the toxic Fragment I sequence (4,550
191 bp) into two sub-fragments, Fragment-I-A and Fragment-I-B, each 2,315-2,316 bp. These sub-
192 fragments were produced via *synthetic clonal genes* using medium copy number bacterial
193 plasmids and amplified in bacteria (**Table S1, Fig 3, File S1**). Transfection of four overlapping
194 ISA DNA fragments generated via *synthetic clonal genes* (**Fig 3**) consistently rescued infectious
195 JEV in all five replicates. The virus induced CPE in all transfected wells at passages 0 and 1 (**Fig**
196 **4A**), as well as in flasks during subsequent passaging and virus stock generation. Sanger
197 sequencing confirmed correct sequences in the JEV stock. The JEV stock produced in VERO-
198 ZAP-KO cells exhibited high infectious titers when titrated on both VERO-ZAP-WT and
199 VERO-ZAP-KO cells (**Fig 4B**), along with high viral RNA loads (**Fig 4C**) and E protein
200 expression (**Fig 4D**).

201 Next, we conducted a mouse study to identify whether JEV obtained with the synthetic ISA
202 approach causes typical infection phenotypes *in vivo*. The SA14-14-2 JEV strain does not cause
203 infection in conventional mice; thus, we used *Ifnar1*$^{-/-}$ mice deficient for the type I IFN receptor
204 function. The wild SA14-14-2 JEV strain causes clinical signs and lethality in *Ifnar1*$^{-/-}$ mice [39].
205 Five-week-old mice, six mice per group, were injected subcutaneously with virus-free media
206 (MOCK) or 10^7 $TCID_{50}$/mouse of the ISA-derived SA14-14-2 JEV. Mice in the MOCK group did
207 not show clinical signs (**Fig 4E**); one MOCK mouse lost weight after manipulation and injection
208 but recovered. Mice in the JEV group showed a high 50% mortality due to paralysis and loss of
209 20% baseline body weight (**Fig 4E**). Another 50% of mice in the JEV group also showed clinical
210 signs—ataxia, depression and hunching but survived.
211
212 We tested spleen and brain from MOCK and JEV groups with the virus-specific RT-qPCR assay.
213 As expected, JEV RNA was not detected in the MOCK group (**Fig 4F**). In contrast, all samples
214 from the JEV groups showed high JEV RNA loads—$10^{5.58-7.52}$ RNA copies per g of the brain, and
215 $10^{5.44-7.60}$ RNA copies per g of the spleen (**Fig 4F**).
216
217 Infection phenotypes in our study with the ISA-derived JEV were comparable to the infection
218 phenotypes in the previous study where *Ifnar1*$^{-/-}$ mice injected with the wild (not synthetic) SA14-
219 14-2 JEV strain also showed mortality, clinical signs, and virus in the spleen [39]. In contrast to
220 our study however, the authors did not find wild SA14-14-2 JEV in the brain. The discrepancy can
221 be explained by the different sampling time—at 12 days after injection in our study, and 4 days in
222 the previous study [39]. Also, in the previous study, mice injected with $10^{6.7}$ plaque forming units
223 (PFU) showed 100% mortality, while mice in our study (10^7 $TCID_{50}$/mouse) showed 50%

224 mortality and 100% morbidity. The difference may be due to different methods to quantify viral
225 loads for injection (PFU versus $TCID_{50}$ assay), the route of injection—intraperitoneal previously
226 and subcutaneous in our study, and potentially reduced viral population complexity in synthetically
227 rescued JEV compared to wild viruses.
228
229 Altogether, dividing the toxic JEV fragment into two sub-fragments provides a highly efficient
230 and robust ISA approach for reverse genetics. This method overcomes the bacterial toxicity caused
231 by JEV sequences and enables the successful rescue of synthetic recombinant JEV.
232

233 **Infectious-Subgenomic-Amplicons methods to overcome bacterial toxicity caused by West**
234 **Nile virus sequences**

235 During the rescue of the wild-type WNV NY99 strain (WNV-WT), Fragment I exhibited
236 bacterial toxicity when using a medium copy bacterial plasmid (**Fig 5**). To address this, a low
237 copy plasmid was utilized (**Fig 5**), which enabled the successful rescue of Fragment I after
238 several attempts over a three-month period.
239

240 As observed with JEV (**Fig 3**), classical ISA failed to rescue the WNV NY99 strain which was
241 permutated (WNV-Per) to generate the permutated control virus (see materials and methods; **File**
242 **S2**, **Table S2**) across three different medium and low copy bacterial plasmids (**Table S1, Fig 6**).
243 To overcome this issue, the toxic Fragment I sequence (4,358 bp) was divided into three sub-
244 fragments: Fragment-I-A (1,198 bp), Fragment-I-B (1,126 bp), and Fragment-I-c (2,179 bp)
245 (**Table S1, File S1**). The first two fragments were made shorter to facilitate bacteria-free

246 *synthesis of DNA* (available only for fragments shorter than 1.8 kb) based on the assumption that
247 the 5' flanking CMV promoter sequence contributed to the toxicity in bacteria. The longer
248 Fragment-I-c was used for *synthetic clonal genes* with medium copy plasmid and bacterial
249 amplification (**Table S1, File S1**). However, due to continued toxicity and failure, Fragment-I-c
250 was further subdivided into overlapping Fragment-I-C (1,162 bp) and Fragment-I-D (1,089 bp),
251 both small enough for bacteria-free *synthesis of DNA*. This troubleshooting led to the six
252 overlapping ISA fragments for WNV-Per (**Fig 6, Table S1, File S1**).

253

254 Transfection of the three overlapping ISA DNA fragments for WNV-WT and six overlapping
255 ISA DNA fragments for WNV-Per consistently rescued the corresponding infectious WNV
256 variants in all five replicates. Sanger sequencing confirmed correct sequences in WNV stocks.
257 Viruses induced CPE in all transfected wells at passages 0 and 1 (**Fig 7A, B**), as well as in flasks
258 during subsequent passaging and virus stock generation. Both WNV-WT and WNV-Per stocks
259 produced in VERO-ZAP-KO cells had high infectious titers when titrated on both VERO-ZAP-
260 WT and VERO-ZAP-KO cells (**Fig 7C, D**), along with high viral RNA loads (**Fig 7C, D**) and E
261 protein expression (**Fig 7E, F**).

262

263 Next, we conducted a mouse study to identify whether WNV-WT and WNV-Per variants obtained
264 with the synthetic ISA approach cause typical infection phenotypes *in vivo*. We used a well-
265 established C57BL/6J mouse model for severe WNV infection [40-42]. Six-week-old C57BL/6J
266 mice (14 mice per group) were MOCK infected or injected intraperitoneally (IP) with 10^7 RNA
267 copies/mouse of WNV-WT or WNV-Per variants. Mice in the MOCK group did not show clinical
268 signs, weight loss, or mortality (**Fig 7G**). Mice in the WNV-WT and WNV-Per groups showed

269 high mortality—93% and 79% (**Fig 7G**), ataxia, depression, paralysis, loss of 20% body weight,
270 and death.
271
272 We tested spleen and brain from MOCK and WNV groups with the virus-specific RT-qPCR assay.
273 As expected, WNV RNA was not detected in the MOCK group (**Fig 7H**). In contrast, all samples
274 from the WNV-WT and WNV-Per groups showed high WNV RNA loads—$10^{4.98-6.97}$ RNA copies
275 per g of the spleen, and $10^{5.78-8.72}$ RNA copies per g of the brain (**Fig 7H**). The difference in viral
276 RNA loads between WNV-WT and WNV-Per groups was not statistically significant ($p < 0.05$),
277 which is expected because permutation in the WNV-Per variant does not affect encoded proteins
278 and does not considerably affect genome coding parameters (**Table S2**).
279
280 Infection phenotypes in our study with the ISA-derived WNV variants were comparable to the
281 infection phenotypes in the previous study where C57BL/6J mice injected with the wild (not
282 synthetic) WNV NY99 strain also showed mortality, clinical signs, and virus in the spleen and
283 brain [40-42].
284
285 **Comparative Infectious-Subgenomic-Amplicons in ZAP wild-type and ZAP knockout cells**
286 The zinc finger antiviral protein 1 (ZAP) exhibits broad-spectrum antiviral activity. Recent
287 studies, including our own, have demonstrated that flaviviruses such as Zika virus, JEV, and
288 WNV are susceptible to ZAP antiviral effects in VERO cells [43-45]. Here, we compared the
289 efficiency of JEV and WNV ISA in wild-type (ZAP-WT) and ZAP knockout (ZAP-KO) cells.
290 We selected JEV and WNV-Per variant, using four and six ISA fragments, respectively (**Figs 3,**
291 **6**) for comparative ISA. Infectious-Subgenomic-Amplicons for each variant were performed

292 concurrently, as described in the supplemental materials and methods, with DNA amplicons for
293 transfection into ZAP-WT or ZAP-KO cells derived from the same PCR reactions.
294
295 Japanese encephalitis virus induced CPE in all five replicates of both ZAP-WT and ZAP-KO
296 cells during passage 0, with more pronounced CPE in ZAP-KO cells (**Fig 8A**). West Nile virus
297 caused extensive CPE in both ZAP-WT and ZAP-KO cells (**Fig 8A**). During passage 1, both
298 JEV and WNV-Per infections in ZAP-KO cells were associated with higher E protein expression
299 compared to ZAP-WT cells ($p < 0.0001$; **Figs 8B, D**). Consequently, JEV and WNV-Per viral
300 RNA loads in supernatants were significantly higher in ZAP-KO cells than in ZAP-WT cells ($p <$
301 0.0001) (**Figs 8C, E**).
302
303 Overall, both wild-type and ZAP knockout cell types demonstrated 100% ISA efficiency,
304 successfully rescuing JEV and WNV in all five replicates. However, ISA in ZAP-KO cells
305 resulted in a higher number of virus-positive cells and elevated viral RNA loads.
306

307 **DISCUSSION**

308 The goal of this study was to validate modified ISA strategies for producing toxic ISA flavivirus
309 fragments synthetically, overcoming bacterial toxicity and eliminating the need to amplify toxic
310 fragments from biological specimens or other preexisting sources. These fully synthetic ISA
311 strategies enable the generation of entirely synthetic JEV and WNV stocks. The strategies
312 involved: (i) Subdividing the problematic toxic DNA fragment into two sub-fragments for
313 subsequent *synthetic clonal gene* production with bacterial plasmids and bacteria. (ii) Using a
314 low copy bacterial plasmid. (iii) Subdividing the toxic DNA fragment into four short overlapping

315 sub-fragments, each up to 1.8 kb, for subsequent bacteria-free *synthesis of DNA* production. To
316 our knowledge, the latter strategy had never been applied for ISA before.
317
318 As expected, and previously demonstrated for the DENV 2 serotype [19], the classical ISA
319 approach of subdividing the flavivirus genome into three overlapping fragments of
320 approximately 4 kb each works well for DENV. These fragments were synthesized quickly and
321 without technical difficulties by a commercial supplier using a medium copy bacterial plasmid
322 (**Table S1**).
323 In contrast, this three-fragment ISA approach failed when we attempted to rescue JEV SA14-14-
324 2 Fragment I using three different medium and low copy bacterial plasmids (**Table S1**). The
325 solution was to divide the toxic fragment into two sub-fragments. We encountered similar
326 technical difficulties producing WNV NY99 Fragment I. Here, replacing the medium copy
327 plasmid with a low copy plasmid resolved the issue, allowing the rescue of the entirely synthetic
328 WNV NY99 variant, but this took several attempts and over three months.
329 More challenging difficulties arose when we attempted to rescue the permuted WNV-Per variant.
330 Similar to JEV ISA, we failed to produce Fragment I using three different medium and low copy
331 bacterial plasmids. Subdividing the toxic Fragment I into three sub-fragments (A, B, and c) did
332 not work because the sub-fragment Fragment I-c was also toxic to bacteria (**Table S1**).
333 Subsequently, we divided the highly toxic WNV Fragment I into four sub-fragments, each
334 smaller than 1.8 kb. This allowed the *synthesis of DNA* commercial production process that is
335 entirely bacteria-free (**Table S1**).
336
337

338 While various approaches have been employed to overcome technical difficulties in constructing
339 cDNA molecules representing the full-length flavivirus genomes in bacterial vectors, this process
340 remains challenging, laborious, and time-consuming. As demonstrated by our difficulties during
341 the rescue of synthetic JEV and WNV (**Table S1**), these challenges are also present in the
342 classical ISA approach. We propose that subdividing toxic fragments into sub-fragments smaller
343 than 1.8 kb suitable for the *synthesis of DNA* process is currently the most rapid and robust
344 strategy to overcome the need for bacterial plasmids and bacteria and ensure the fast rescue of
345 entirely synthetic flaviviruses.
346 This strategy significantly shortens the time required to produce recombinant flaviviruses. For
347 example, the *synthesis of DNA* process by a commercial supplier (**Table S1**) has turnaround time
348 2-4 days. Additionally, the synthesis of DNA is cost-effective with current 0.07 USD per bp; for
349 example, 4.3 kb DNA fragment for WNV ISA ordered via *synthetic clonal genes* process with
350 bacterial plasmids and amplification in bacteria costs around 840 USD with 3-4 weeks
351 turnaround time, while the same fragment divided into three sub-fragments and ordered via
352 bacteria-free *synthesis of DNA* costs 360 USD with 2-4 days turnaround time. During production,
353 the provider flanks DNA fragments with short 22 bp adapters (**File S1**), facilitating efficient PCR
354 amplification of ordered ISA fragments from the provided construct. The provider also applies
355 NGS to verify correct sequences, reducing both time and costs for virus rescue. We anticipate
356 that ongoing improvements in DNA synthesis technology and associated cost reductions will
357 provide even faster and more cost-effective bacteria-free fragments for ISA, enabling the even
358 more rapid production of entirely synthetic flaviviruses.
359

360 The zinc finger CCCH-type antiviral protein 1, also known as ZAP, ZC3HAV1, or PARP13, is a
361 cellular protein with broad antiviral activity. ZAP binds viral RNA and evokes antiviral activity
362 by mediating viral RNA degradation and translational inhibition [46]. It also interacts with
363 various cellular proteins that may act as co-factors, enhancing its antiviral effects [47].
364 Furthermore, ZAP can augment other antiviral systems [43,48]. Recent studies, including our
365 own, have demonstrated that flaviviruses such as Zika virus, JEV, and WNV are susceptible to
366 ZAP antiviral effects in VERO cells [43-45]. Thus, we also compared the efficacy of JEV and
367 WNV ISA in ZAP-WT and ZAP-KO cells. Both cell types showed 100% efficiency, with viruses
368 successfully rescued in all five replicates. However, the increased number of virus-positive cells
369 in ZAP-KO cells suggests that these cells may be more effective for rescuing modified
370 flaviviruses, such as attenuated variants for live attenuated vaccines [27,28].

371

372 In conclusion, the ISA method is a robust and straightforward approach to reverse genetics for
373 JEV and WNV. In this study, we validated a modified ISA strategy that involves subdividing the
374 toxic DNA fragment into four short overlapping sub-fragments, each up to 1.8 kb, for subsequent
375 bacteria-free *DNA synthesis* production. To our knowledge, this strategy had never been applied
376 to ISA before, enabling the rapid generation of JEV and WNV using a completely synthetic
377 method for toxic ISA flavivirus fragments. The strategy can be particularly beneficial for
378 research on emerging flaviviruses where a rapid response is needed to rescue new virus variants
379 during outbreaks.

380

381

DISCLOSURE STATEMENT

The authors declare that the research was conducted in the absence of any commercial or financial relationships that could be construed as a potential conflict of interest.

AUTHOR CONTRIBUTIONS

Conceptualization: PPS, NPKL, UK. Investigation: PPS, NPKL, UK. Data analysis: PPS, NPKL, UK. Funding: UK. Writing—original draft preparation: PPS, NPKL, UK. Writing—review and editing: PPS, NPKL, UK.

DATA AVAILABILITY

All data are available in the manuscript or in the supplemental data.

FUNDING

PPS received a Scholarship from the School of Public Health, University of Saskatchewan. The funder had no role in study design, data collection and analysis, decision to publish, or manuscript preparation.

407 **REFERENCES**

408 1. Pierson TC, Diamond MS. The continued threat of emerging flaviviruses. Nat Microbiol. 2020
409 Jun;5(6):796-812.
410 2. Blackburn NK, Swanepoel R. An investigation of flavivirus infections of cattle in Zimbabwe
411 Rhodesia with particular reference to Wesselsbron virus. J Hyg (Lond). 1980 Aug;85(1):1-33.
412 3. Bhatt S, Gething PW, Brady OJ, et al. The global distribution and burden of dengue. Nature. 2013
413 Apr 25;496(7446):504-7.
414 4. Gubler DJ. Dengue/dengue haemorrhagic fever: history and current status. Novartis Found
415 Symp. 2006;277:3-16; discussion 16-22, 71-3, 251-3.
416 5. Amicizia D, Zangrillo F, Lai PL, et al. Overview of Japanese encephalitis disease and its prevention.
417 Focus on IC51 vaccine (IXIARO®). Journal of Preventive Medicine and Hygiene2018. p. E99-E107.
418 6. Tarantola A, Goutard F, Newton P, et al. Estimating the burden of Japanese encephalitis virus and
419 other encephalitides in countries of the mekong region. In: Gray DJ, editor. PLoS neglected
420 tropical diseases2014. p. e2533.
421 7. Chaturvedi UC, Mathur A, Chandra A, et al. Transplacental Infection with Japanese Encephalitis
422 Virus. Journal of Infectious Diseases: Oxford University Press; 1980. p. 712-715.
423 8. Lindquist L. Recent and historical trends in the epidemiology of Japanese encephalitis and its
424 implication for risk assessment in travellers. Journal of Travel Medicine2018. p. S3-S9.
425 9. Oliveira ARS, Piaggio J, Cohnstaedt LW, et al. Introduction of the Japanese encephalitis virus (JEV)
426 in the United States – A qualitative risk assessment. Transboundary and Emerging Diseases2019.
427 p. 1558-1574.
428 10. Huang YJS, Harbin JN, Hettenbach SM, et al. Susceptibility of a North American Culex
429 quinquefasciatus to Japanese Encephalitis Virus. Vector borne and zoonotic diseases (Larchmont,
430 N.Y.): Vector Borne Zoonotic Dis; 2015. p. 709-711.
431 11. Faizah AN, Kobayashi D, Matsumura R, et al. Blood meal source identification and RNA virome
432 determination in Japanese encephalitis virus vectors collected in Ishikawa Prefecture, Japan,
433 show distinct avian/mammalian host preference. J Med Entomol. 2023 Apr 7.
434 12. Shimizu T, Kawakami Y, Fukuhara S, et al. Experimental stillbirth in pregnant swine infected with
435 Japanese encephalitis virus. The Japanese journal of experimental medicine1954. p. 363-375.
436 13. Howard-Jones AR, Pham D, Jeoffreys N, et al. Emerging Genotype IV Japanese Encephalitis Virus
437 Outbreak in New South Wales, Australia. Viruses. 2022 Aug 24;14(9).
438 14. Barrett ADT. West Nile in Europe: an increasing public health problem. J Travel Med. 2018 Jan
439 1;25(1).
440 15. Petersen LR, Carson PJ, Biggerstaff BJ, et al. Estimated cumulative incidence of West Nile virus
441 infection in US adults, 1999-2010. Epidemiol Infect. 2013 Mar;141(3):591-5.
442 16. Neumann G, Kawaoka Y. Reverse genetics systems for the generation of segmented negative-
443 sense RNA viruses entirely from cloned cDNA. Curr Top Microbiol Immunol. 2004;283:43-60.
444 17. Aubry F, Nougairede A, Gould EA, et al. Flavivirus reverse genetic systems, construction
445 techniques and applications: a historical perspective. Antiviral Res. 2015 Feb;114:67-85.
446 18. Ruggli N, Rice CM. Functional cDNA clones of the Flaviviridae: strategies and applications. Adv
447 Virus Res. 1999;53:183-207.
448 19. Park CJ, Lee YA, Yoo SM, et al. Efficient reverse genetics approach involving infectious
449 subgenomic amplicon for engineering dengue virus. J Med Virol. 2023 Aug;95(8):e28978.
450 20. Gritsun TS, Gould EA. Infectious transcripts of tick-borne encephalitis virus, generated in days by
451 RT-PCR. Virology. 1995 Dec 20;214(2):611-8.
452 21. Rice CM, Grakoui A, Galler R, et al. Transcription of infectious yellow fever RNA from full-length
453 cDNA templates produced by in vitro ligation. New Biol. 1989 Dec;1(3):285-96.

454 22. Kapoor M, Zhang L, Mohan PM, et al. Synthesis and characterization of an infectious dengue
455 virus type-2 RNA genome (New Guinea C strain). Gene. 1995 Sep 11;162(2):175-80.
456 23. Sumiyoshi H, Hoke CH, Trent DW. Infectious Japanese encephalitis virus RNA can be synthesized
457 from in vitro-ligated cDNA templates. J Virol. 1992 Sep;66(9):5425-31.
458 24. Aubry F, Nougairède A, de Fabritus L, et al. Single-stranded positive-sense RNA viruses generated
459 in days using infectious subgenomic amplicons. The Journal of general virology2014. p. 2462-7.
460 25. Cochin M, Driouich JS, Moureau G, et al. In vivo rescue of arboviruses directly from subgenomic
461 DNA fragments. Emerg Microbes Infect. 2024 Dec;13(1):2356140.
462 26. Trus I, Berube N, Jiang P, et al. Zika Virus with Increased CpG Dinucleotide Frequencies Shows
463 Oncolytic Activity in Glioblastoma Stem Cells. Viruses: Multidisciplinary Digital Publishing
464 Institute; 2020. p. 579.
465 27. Trus I, Udenze D, Berube N, et al. CpG-Recoding in Zika Virus Genome Causes Host-Age-
466 Dependent Attenuation of Infection With Protection Against Lethal Heterologous Challenge in
467 Mice. Front Immunol. 2019;10:3077.
468 28. Trus I, Udenze D, Karniychuk U. Generation of CpG-Recoded Zika Virus Vaccine Candidates.
469 Methods in molecular biology (Clifton, N.J.): Methods Mol Biol; 2022. p. 289-302.
470 29. Udenze D, Trus I, Berube N, et al. CpG content in the Zika virus genome affects infection
471 phenotypes in the adult brain and fetal lymph nodes. Front Immunol. 2022;13:943481.
472 30. Hu F, Zhu T, Guo X, et al. Generation of duck Tembusu virus using a simple reverse genetic system
473 in duck embryo fibroblast cells. J Virol Methods. 2022 Feb;300:114385.
474 31. Hoornweg TE, Godeke GJ, Hoogerwerf MN, et al. Rescue and in vitro characterization of a
475 divergent TBEV-Eu strain from the Netherlands. Sci Rep. 2023 Feb 18;13(1):2872.
476 32. Atieh T, Nougairède A, Klitting R, et al. New reverse genetics and transfection methods to rescue
477 arboviruses in mosquito cells. Scientific Reports: Nature Publishing Group; 2017. p. 13983.
478 33. Driouich JS, Moureau G, de Lamballerie X, et al. Reverse Genetics of RNA Viruses: ISA-Based
479 Approach to Control Viral Population Diversity without Modifying Virus Phenotype. Viruses. 2019
480 Jul 20;11(7).
481 34. Atieh T, Baronti C, de Lamballerie X, et al. Simple reverse genetics systems for Asian and African
482 Zika viruses. Scientific reports: Nature Publishing Group; 2016. p. 39384.
483 35. Touret F, Gilles M, Klitting R, et al. Live Zika virus chimeric vaccine candidate based on a yellow
484 fever 17-D attenuated backbone. Emerg Microbes Infect. 2018 Sep 26;7(1):161.
485 36. Klitting R, Roth L, Rey FA, et al. Molecular determinants of Yellow Fever Virus pathogenicity in
486 Syrian Golden Hamsters: one mutation away from virulence. Emerg Microbes Infect. 2018 Mar
487 29;7(1):51.
488 37. Fiacre L, Nougairede A, Migne C, et al. Different viral genes modulate virulence in model
489 mammal hosts and Culex pipiens vector competence in Mediterranean basin lineage 1 West Nile
490 virus strains. Front Microbiol. 2023;14:1324069.
491 38. Aubry F, Nougairède A, de Fabritus L, et al. “ISA-Lation” of Single-Stranded Positive-Sense RNA
492 Viruses from Non-Infectious Clinical/Animal Samples. In: Ng LFP, editor. PLOS ONE: Public Library
493 of Science; 2015. p. e0138703.
494 39. Liu J, Jing W, Fang Y, et al. The Infection of the Japanese Encephalitis Virus SA14-14-2 Strain
495 Induces Lethal Peripheral Inflammatory Responses in IFNAR Deficiency Mice. Frontiers in
496 microbiology: Front Microbiol; 2022.
497 40. Zhang YN, Li N, Zhang QY, et al. Rational design of West Nile virus vaccine through large
498 replacement of 3' UTR with internal poly(A). EMBO Mol Med. 2021 Sep 7;13(9):e14108.
499 41. Daffis S, Samuel MA, Keller BC, et al. Cell-specific IRF-3 responses protect against West Nile virus
500 infection by interferon-dependent and -independent mechanisms. PLoS Pathog. 2007 Jul
501 27;3(7):e106.

42. Daffis S, Samuel MA, Suthar MS, et al. Interferon regulatory factor IRF-7 induces the antiviral alpha interferon response and protects against lethal West Nile virus infection. J Virol. 2008 Sep;82(17):8465-75.
43. Nguyen Phuong Khanh Le PPS, Ahmad Jawad Sabir, Ivan Trus, Uladzimir Karniychuk. Endogenous ZAP is associated with altered global cellular gene expression during Zika virus infection. bioRxiv. 2024.
44. Chiu HP, Chiu H, Yang CF, et al. Inhibition of Japanese encephalitis virus infection by the host zinc-finger antiviral protein. PLoS Pathogens: Public Library of Science; 2018.
45. Ahmad Jawad Sabir NPKL, Prince Pal Singh, Uladzimir Karniychuk. Endogenous ZAP affects Zika virus RNA interactome. bioRxiv. 2024.
46. Li MMH, Aguilar EG, Michailidis E, et al. Characterization of Novel Splice Variants of Zinc Finger Antiviral Protein (ZAP). J Virol. 2019 Sep 15;93(18).
47. Goodier JL, Pereira GC, Cheung LE, et al. The Broad-Spectrum Antiviral Protein ZAP Restricts Human Retrotransposition. PLOS Genetics: Public Library of Science; 2015. p. e1005252.
48. Nguyen LP, Aldana KS, Yang E, et al. Alphavirus Evasion of Zinc Finger Antiviral Protein (ZAP) Correlates with CpG Suppression in a Specific Viral nsP2 Gene Sequence. Viruses. 2023 Mar 24;15(4).

538 **FIGURE LEGENDS**

539 **Figure 1. Classical ISA method for dengue virus.**
540
541
542 **Figure 2. Dengue virus ISA and stock generation**. (**A**) Cytopathic effect in DENV ISA-
543 transfected ZAP-KO BHK+VERO cells, passage 0 day 7 after transfection. All five replicate wells
544 showed CPE at passages 0 and 1; the representative images are shown. (**B**) Infectious $TCID_{50}$ titers
545 of the DENV stock produced in ZAP-KO cells. The stock was titrated in VERO-ZAP-WT or
546 VERO-ZAP-KO cells. (**C**) DENV RNA loads of the stock determined by virus-specific RT-qPCR.
547 (**D**) Images of cells positive for the DENV E protein (red staining) at 7 days after infection with
548 MOI 0.01. Magnification x200. The experiment was done in 4 replicates. Figures represent the
549 general patterns in all replicates.
550
551
552 **Figure 3. The adapted ISA method for Japanese encephalitis virus.** To overcome toxicity we
553 divided the toxic Fragment I into two sub-fragments (**Table S1**, **File S1**).
554
555
556 **Figure 4. JEV ISA and stock generation**. (**A**) Cytopathic effect in JEV SA14-14-2 ISA-
557 transfected ZAP-KO BHK+VERO cells, passage 0, day 6 after transfection. All five replicates
558 showed CPE; the representative images are shown. (**B**) Infectious $TCID_{50}$ titers of the JEV stock
559 produced in ZAP-KO cells. The stock was titrated in VERO-ZAP-WT or VERO-ZAP-KO cells.
560 (**C**) JEV RNA loads of the stock determined by virus-specific RT-qPCR. (**D**) Images of cells
561 positive for the JEV E protein (red staining) at 3 days after infection, MOI 0.01. Magnification
562 x200. The experiment was done in 3 biological replicates. Figures represent the general patterns
563 in replicates. (**E**) Mean body weight and survival in MOCK *Ifnar1*$^{-/-}$ mice and *Ifnar1*$^{-/-}$ mice
564 injected with the ISA-derived JEV SA14-14-2. The following clinical scoring was used: 0—no
565 visible abnormalities; 1—mild ataxia or tremors; 2—obvious ataxia or tremors; 3—depression,
566 hunching, reluctance to walk, and falling to the side when walking; 4—close to moribund but still
567 somewhat responsive; 5—paralysis; 6—loos of 20% baseline body weight; 7—found dead. Scores
568 4, 5, or 6 were used for the endpoint and mouse euthanasia. In body weight a standard error of the
569 mean (SEM) is shown. (**F**) JEV loads in mouse spleen and brain sampled at euthanasia due to
570 severe clinical signs or at the end of the study—at 12 days after injection.
571
572
573
574 **Figure 5. The adapted ISA method for the wild-type WNV variant (WNV-WT).** To
575 overcome toxicity, we generated Fragment I in the low copy pCC1 bacterial plasmid (**Table S1**,
576 **File S1**).
577
578
579
580 **Figure 6. The adapted ISA method for the permuted WNV variant (WNV-Per).** To
581 overcome toxicity, we subdivide the toxic Fragment I into four sub-fragments for bacteria-free
582 *synthesis of DNA* production (**Table S1**, **File S1**).
583

584 **Figure 7. WNV ISA and stock generation**. Cytopathic effect in WNV-WT (**A**) and WNV-Per
585 (**B**) ISA-transfected ZAP-KO BHK+VERO cells, passage 0, day 6 after transfection. All five
586 replicates for each WNV variant showed CPE; representative images are shown. Infectious $TCID_{50}$
587 titers and RT-qPCR RNA loads of the WNV-WT (**C**) and WNV-Per (**D**) stocks produced in ZAP-
588 KO cells. For $TCID_{50}$ virus stocks were titrated in VERO-ZAP-WT or VERO-ZAP-KO cells.
589 Images of cells positive for the WNV-WT (**E**) and WNV-Per (**F**) E protein (red staining) at 3 days
590 after infection, MOI 0.01. Magnification x200. The experiment was done in 3 biological replicates.
591 Figures represent the general patterns in all replicates. (**G**) Mean body weight and survival in
592 MOCK C57BL/6J mice and C57BL/6J mice injected with the ISA-derived WNV-WT and WNV-
593 Per. The following clinical scoring was used: 0—no visible abnormalities; 1—mild ataxia or
594 tremors; 2—obvious ataxia or tremors; 3—depression, hunching, reluctance to walk, and falling
595 to the side when walking; 4—close to moribund but still somewhat responsive; 5—paralysis; 6—
596 loos of 20% baseline body weight; 7—found dead. Scores 4, 5, or 6 were used for the endpoint
597 and mouse euthanasia. In body weight a standard error of the mean (SEM) is shown. (**H**) WNV
598 loads in mouse spleen and brain sampled at euthanasia due to severe clinical signs or at the end of
599 the study—at 14 days after injection.
600
601
602 **Figure 8. Comparative ISA in ZAP-WT and ZAP-KO cells**. (**A**) Cytopathic effect in JEV and
603 WNV-Per ISA-transfected ZAP-WT and ZAP-KO BHK+VERO cells, passage 0, day 5 (JEV) and
604 day 4 (WNV-Per) after transfection. All five replicates for JEV and WNV-Per showed CPE; the
605 representative images are shown. The digital quantification of JEV (**B**) and WNV-Per (**D**) E
606 protein-positive cells in all 5-well replicates at day 4 (JEV) and day 2 (WNV-Per) during passage
607 1 of comparative ISA. For technical replicates, three random images were obtained from each well.
608 Examples of JEV and WNV-Per E protein IHC are in **Figures 4D** and **7F**. JEV (**C**) and WNV-Per
609 (**E**) RNA loads in supernatants collected at day 4 (JEV) and day 2 (WNV-Per) during passage 1 of
610 comparative ISA. Data from 5-well replicates are shown. ***P***: Unpaired t-test.
611
612
613
614 **SUPPORTING INFORMATION CAPTIONS**
615
616
617 **Supplemental materials and methods**.
618
619
620 **Table S1** ISA fragments and primers.
621
622
623 **Table S2** West Nile virus genomic parameters.
624
625
626 **File S1** ISA fragments.
627
628
629 **File S2** WNV-Permuted reference sequence.

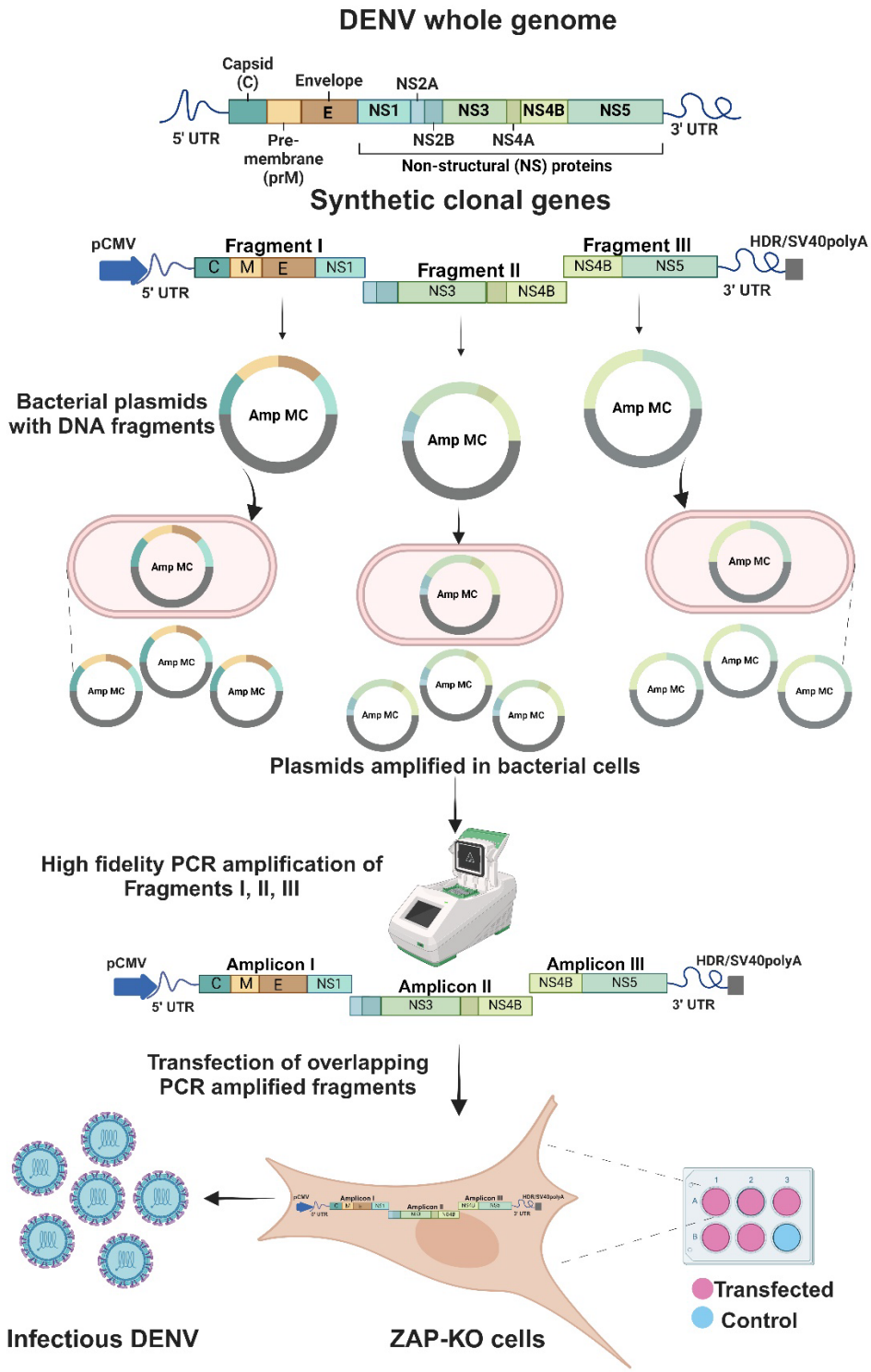
DENV whole genome
Capsid (C)
Envelope
NS2A
E
NS1
NS3
NS4B
NS5
5' UTR
3' UTR
Pre-membrane (prM)
NS2B
NS4A
Non-structural (NS) proteins
Synthetic clonal genes
pCMV
Fragment I
C
M
E
NS1
5' UTR
Fragment II
NS3
NS4B
Fragment III
NS4B
NS5
HDR/SV40polyA
3' UTR
Bacterial plasmids with DNA fragments
Amp MC
Plasmids amplified in bacterial cells
High fidelity PCR amplification of Fragments I, II, III
Amplicon I
Amplicon II
Amplicon III
Transfection of overlapping PCR amplified fragments
Infectious DENV
ZAP-KO cells
Transfected
Control

Fig 1.

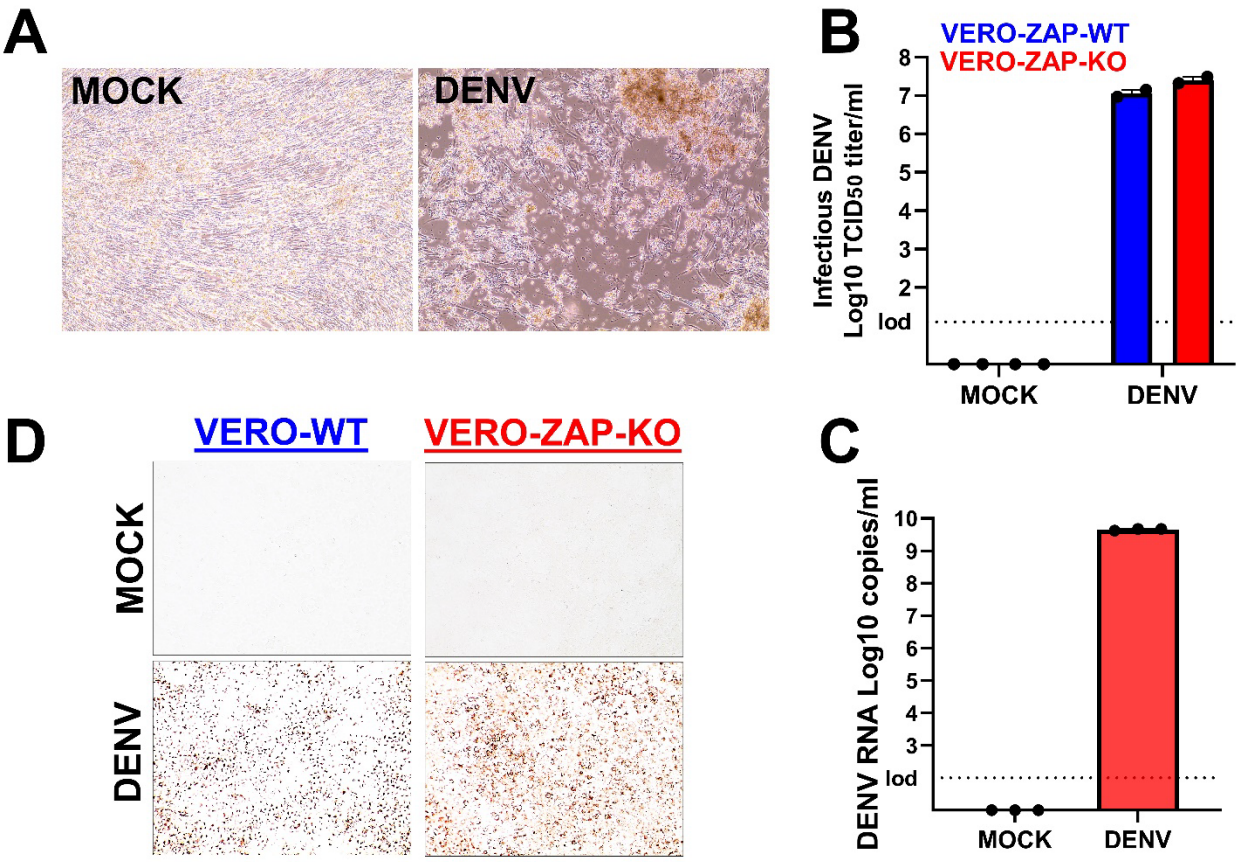
A
MOCK
DENV
B
VERO-ZAP-WT
VERO-ZAP-KO
Infectious DENV
Log10 TCID50 titer/ml
8
7
6
5
4
3
2
lod
MOCK
DENV
D
VERO-WT
VERO-ZAP-KO
MOCK
DENV
C
DENV RNA Log10 copies/ml
10
9
8
7
6
5
4
3
lod
MOCK
DENV

Fig 2.

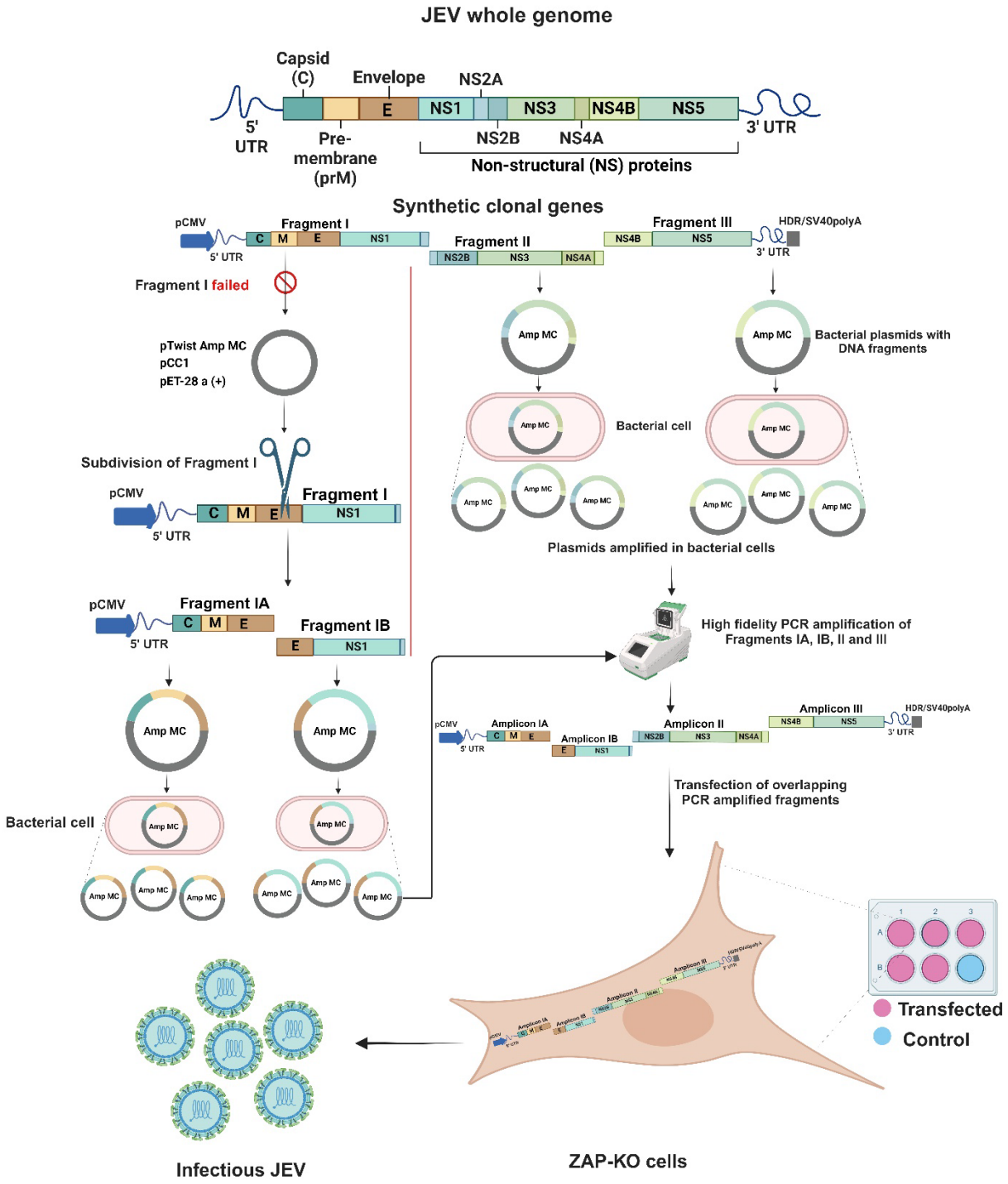
JEV whole genome
Capsid (C)
Envelope
NS2A
5' UTR
Pre-membrane (prM)
E
NS1
NS3
NS4B
NS5
NS2B
NS4A
3' UTR
Non-structural (NS) proteins
Synthetic clonal genes
pCMV
Fragment I
C
M
E
NS1
5' UTR
Fragment II
NS2B
NS3
NS4A
Fragment III
NS4B
NS5
HDR/SV40polyA
3' UTR
Fragment I failed
pTwist Amp MC
pCC1
pET-28 a (+)
Subdivision of Fragment I
Fragment IA
Fragment IB
Amp MC
Bacterial cell
Bacterial plasmids with DNA fragments
Plasmids amplified in bacterial cells
High fidelity PCR amplification of Fragments IA, IB, II and III
Amplicon IA
Amplicon IB
Amplicon II
Amplicon III
Transfection of overlapping PCR amplified fragments
Transfected
Control
Infectious JEV
ZAP-KO cells

Fig 3.

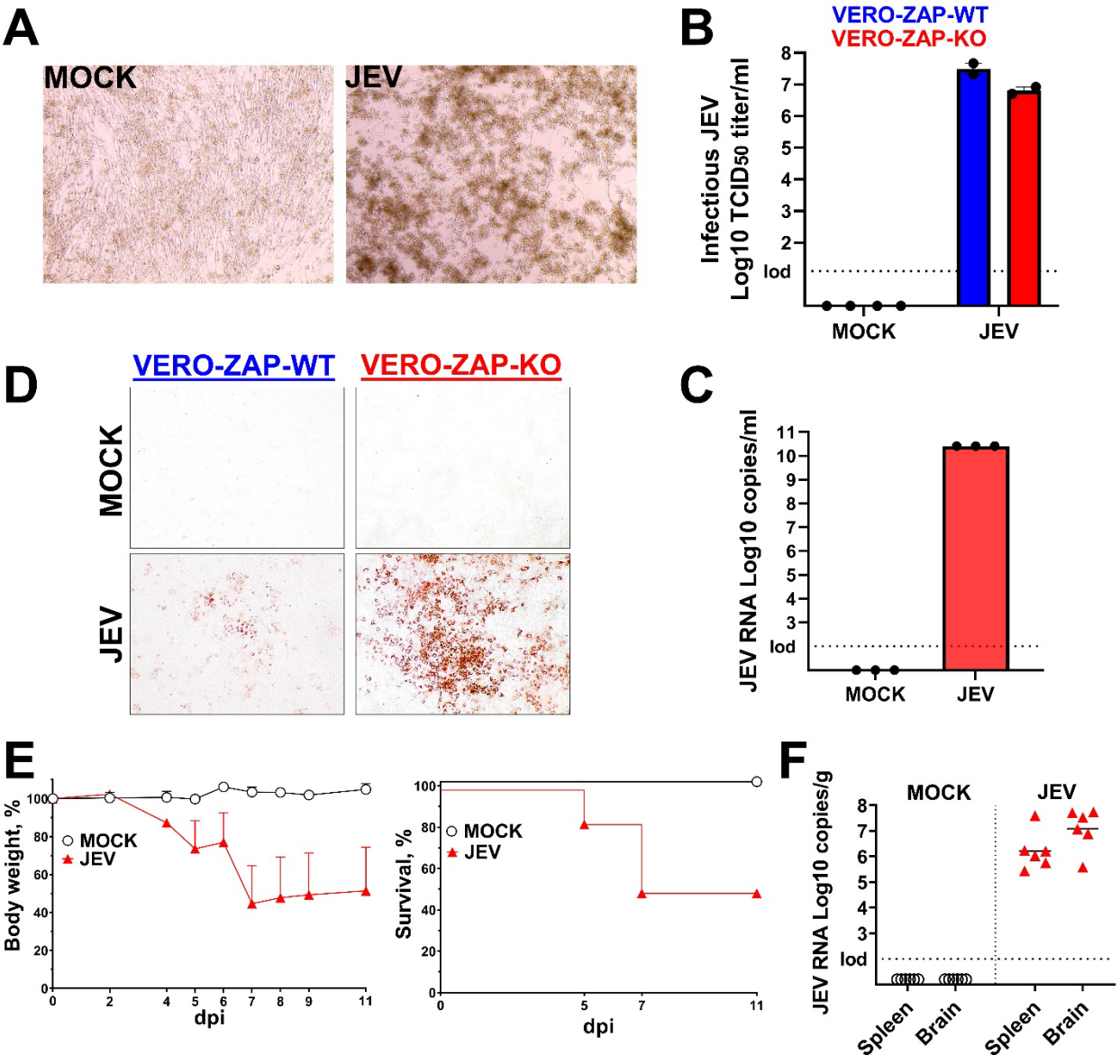
A
MOCK
JEV
B
VERO-ZAP-WT
VERO-ZAP-KO
Infectious JEV
Log10 TCID50 titer/ml
lod
MOCK
JEV
D
VERO-ZAP-WT
VERO-ZAP-KO
MOCK
JEV
C
JEV RNA Log10 copies/ml
lod
MOCK
JEV
E
Body weight, %
MOCK
JEV
dpi
Survival, %
MOCK
JEV
dpi
F
JEV RNA Log10 copies/g
MOCK
JEV
lod
Spleen
Brain
Spleen
Brain

Fig 4.

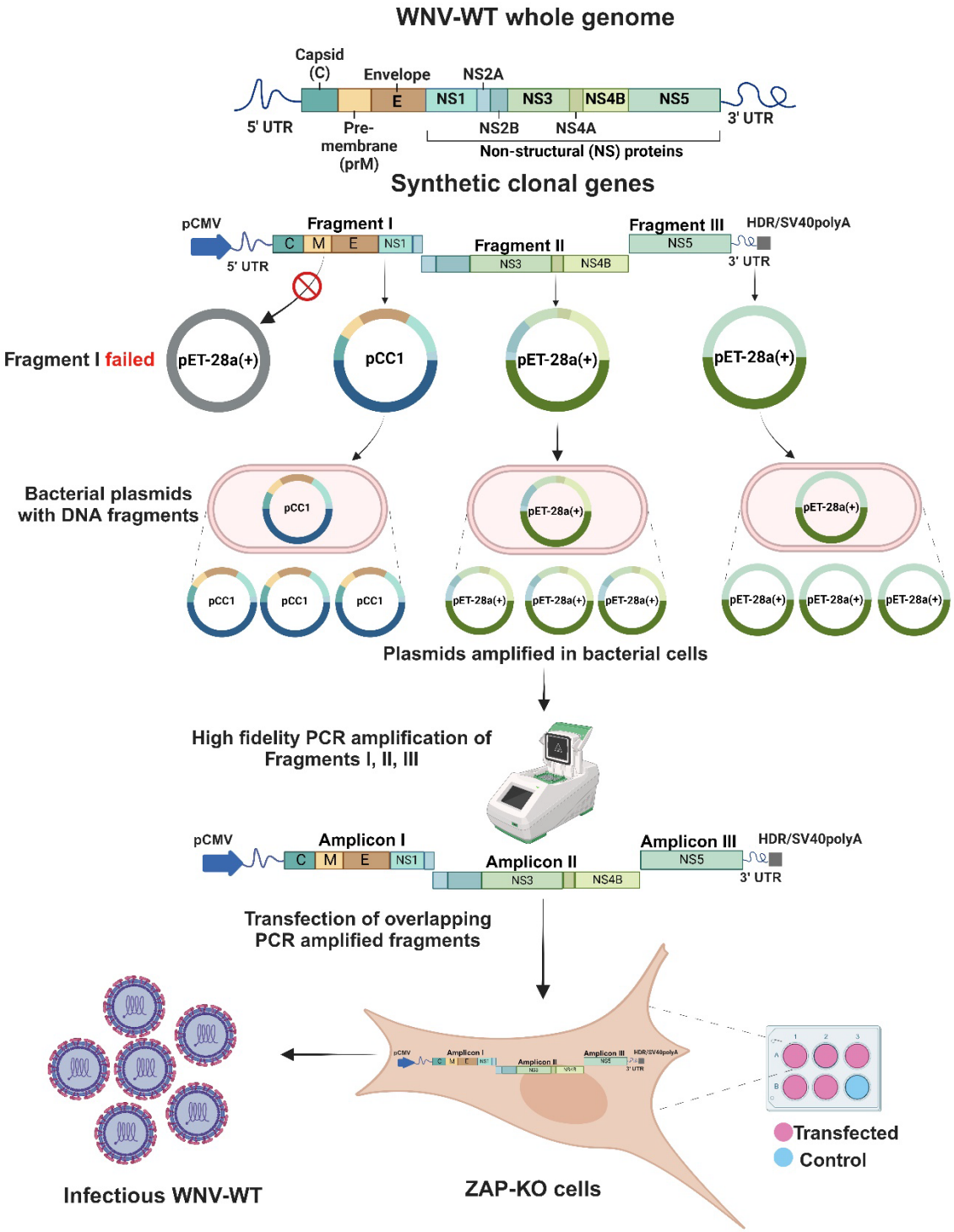
WNV-WT whole genome
Capsid (C)
Envelope
NS2A
E
NS1
NS3
NS4B
NS5
5' UTR
Pre-membrane (prM)
NS2B
NS4A
3' UTR
Non-structural (NS) proteins
Synthetic clonal genes
pCMV
Fragment I
C
M
E
NS1
5' UTR
Fragment II
NS3
NS4B
Fragment III
NS5
HDR/SV40polyA
3' UTR
Fragment I failed
pET-28a(+)
pCC1
pET-28a(+)
pET-28a(+)
Bacterial plasmids with DNA fragments
pCC1
pET-28a(+)
pET-28a(+)
pCC1
pCC1
pCC1
pET-28a(+)
pET-28a(+)
pET-28a(+)
pET-28a(+)
pET-28a(+)
pET-28a(+)
Plasmids amplified in bacterial cells
High fidelity PCR amplification of Fragments I, II, III
pCMV
Amplicon I
C
M
E
NS1
Amplicon II
NS3
NS4B
Amplicon III
NS5
HDR/SV40polyA
3' UTR
Transfection of overlapping PCR amplified fragments
Transfected
Control
Infectious WNV-WT
ZAP-KO cells

Fig 5.

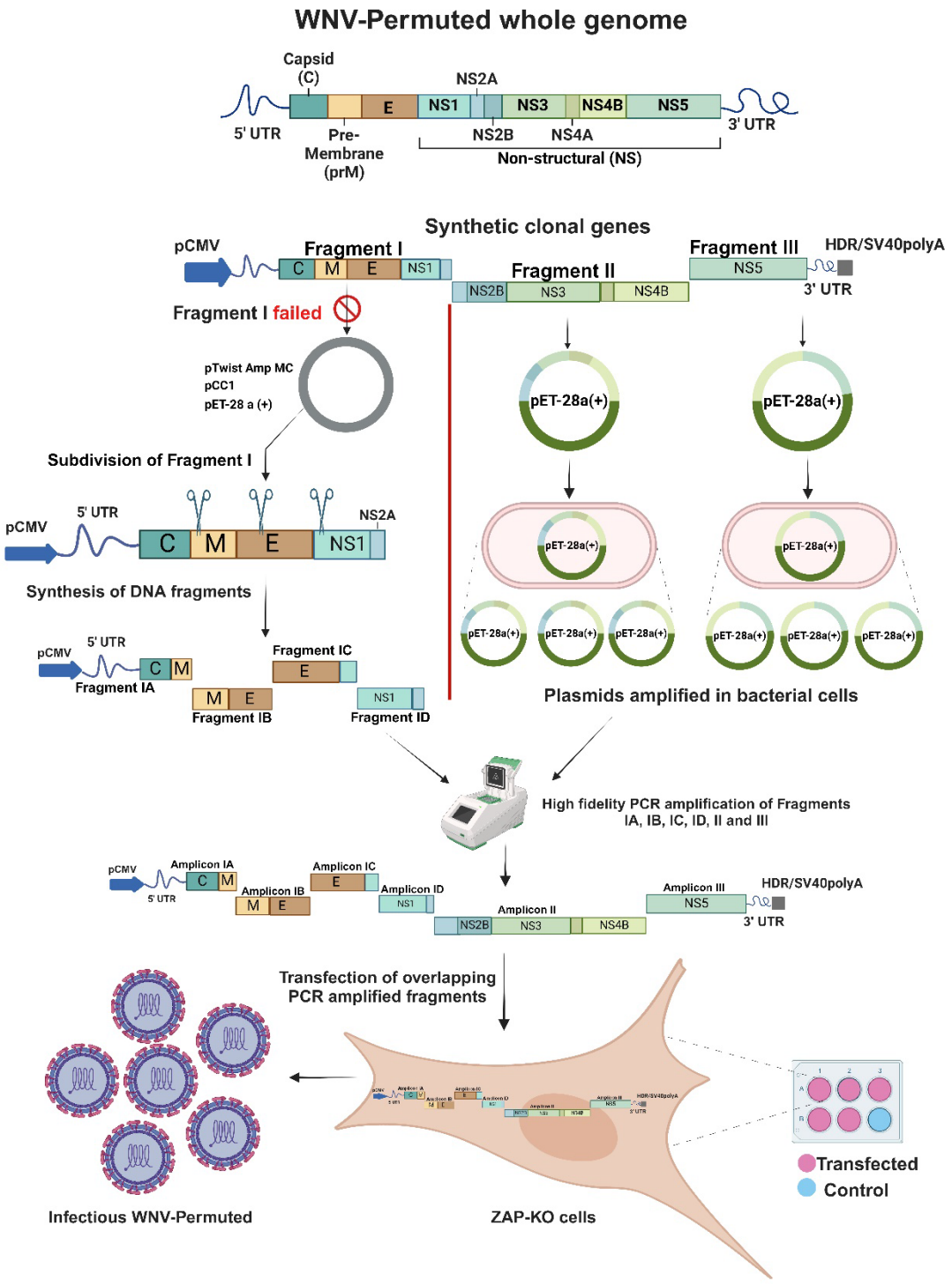
WNV-Permuted whole genome
Capsid (C)
NS2A
5' UTR
Pre-Membrane (prM)
E
NS1
NS3
NS4B
NS5
3' UTR
NS2B
NS4A
Non-structural (NS)
Synthetic clonal genes
pCMV
Fragment I
C
M
E
NS1
Fragment II
NS2B
NS3
NS4B
Fragment III
NS5
HDR/SV40polyA
3' UTR
Fragment I failed
pTwist Amp MC
pCC1
pET-28 a (+)
pET-28a(+)
Subdivision of Fragment I
5' UTR
NS2A
Synthesis of DNA fragments
Fragment IA
Fragment IB
Fragment IC
Fragment ID
Plasmids amplified in bacterial cells
High fidelity PCR amplification of Fragments IA, IB, IC, ID, II and III
Amplicon IA
Amplicon IB
Amplicon IC
Amplicon ID
Amplicon II
Amplicon III
Transfection of overlapping PCR amplified fragments
Transfected
Control
Infectious WNV-Permuted
ZAP-KO cells

Fig 6.

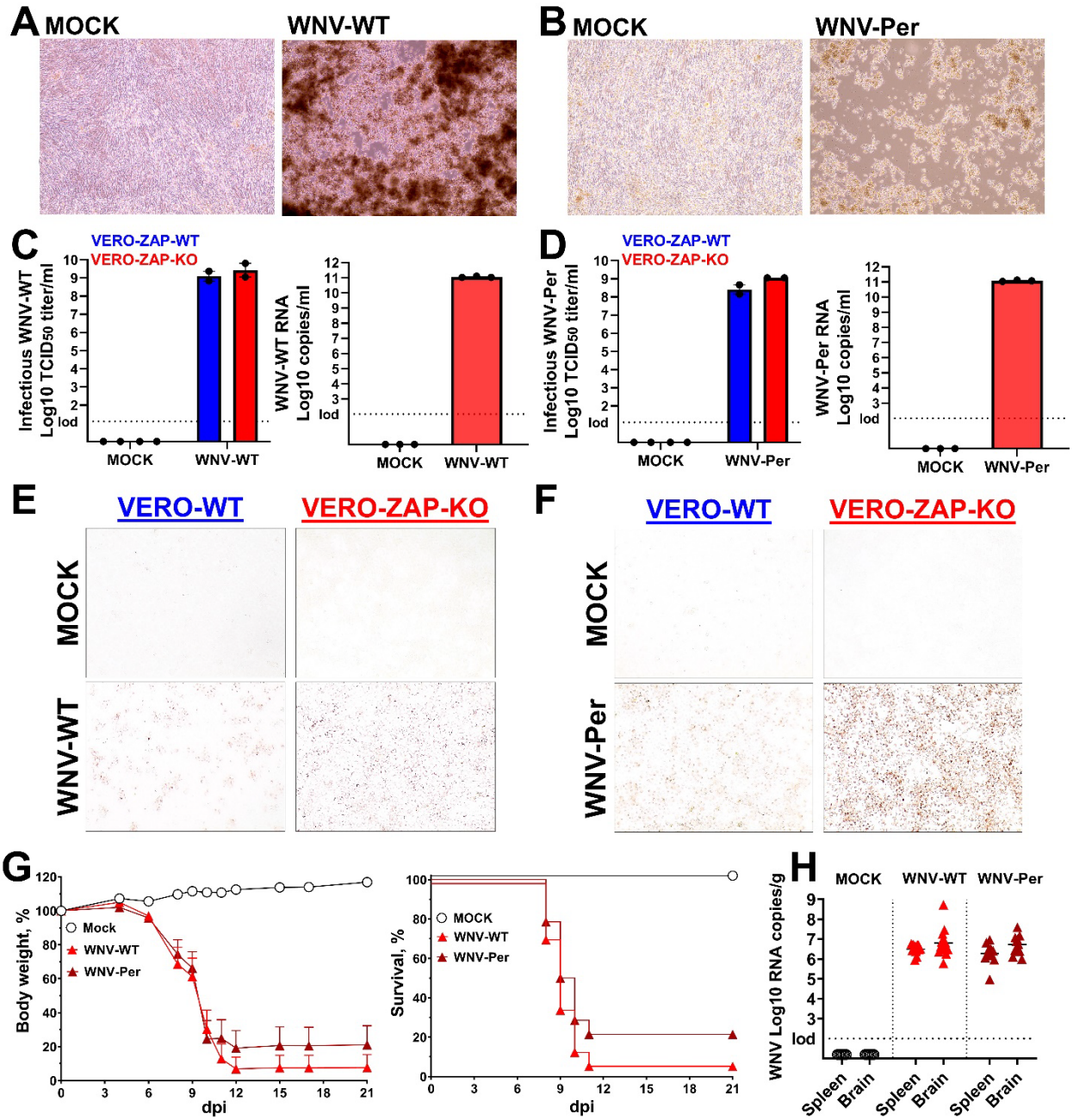
A MOCK
WNV-WT
B MOCK
WNV-Per
C
VERO-ZAP-WT
VERO-ZAP-KO
Infectious WNV-WT Log10 TCID50 titer/ml
lod
MOCK
WNV-WT
WNV-WT RNA Log10 copies/ml
D
Infectious WNV-Per Log10 TCID50 titer/ml
WNV-Per
WNV-Per RNA Log10 copies/ml
E
VERO-WT
VERO-ZAP-KO
MOCK
WNV-WT
F
WNV-Per
G
Body weight, %
Mock
dpi
Survival, %
MOCK
H
WNV Log10 RNA copies/g
Spleen
Brain

Fig 7.

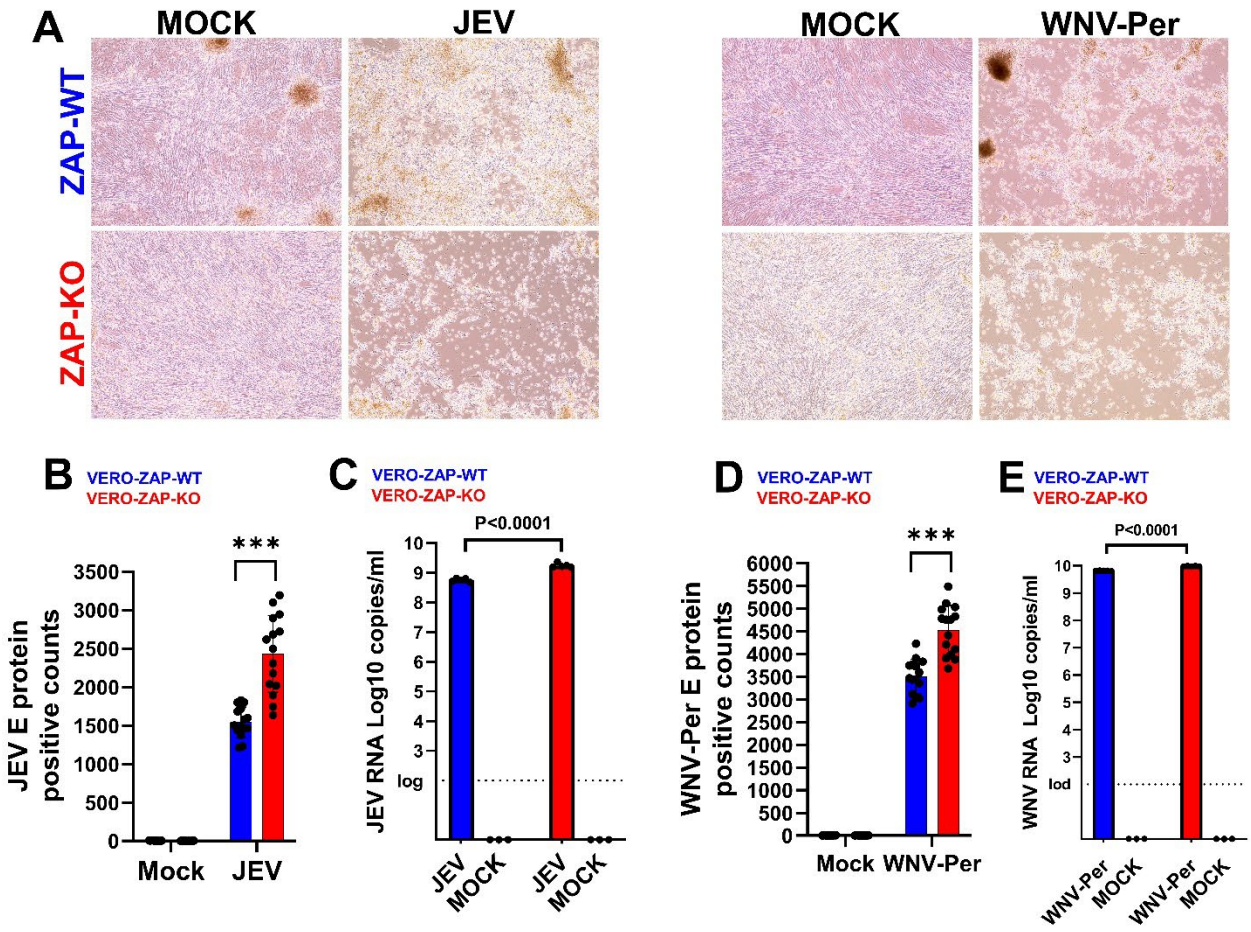
A
MOCK
JEV
MOCK
WNV-Per
ZAP-WT
ZAP-KO
B
VERO-ZAP-WT
VERO-ZAP-KO
***
JEV E protein positive counts
3500
3000
2500
2000
1500
1000
500
0
Mock
JEV
C
VERO-ZAP-WT
VERO-ZAP-KO
P<0.0001
JEV RNA Log10 copies/ml
10
9
8
7
6
5
4
3
log
JEV
MOCK
JEV
MOCK
D
VERO-ZAP-WT
VERO-ZAP-KO
***
WNV-Per E protein positive counts
6000
5500
5000
4500
4000
3500
3000
2500
2000
1500
1000
500
0
Mock
WNV-Per
E
VERO-ZAP-WT
VERO-ZAP-KO
P<0.0001
WNV RNA Log10 copies/ml
10
9
8
7
6
5
4
3
lod
WNV-Per
MOCK
WNV-Per
MOCK

Fig 8.

Infectious subgenomic amplicon strategies for Japanese encephalitis and West Nile viruses

Prince Pal Singh[1,2], Nguyen Phuong Khanh Le[1], Uladzimir Karniychuk[1,*]

[1]Department of Veterinary Biosciences, College of Veterinary Medicine, The Ohio State University, Columbus, OH, USA

[2]School of Public Health, University of Saskatchewan, Saskatoon, Canada

***Correspondence:** Uladzimir Karniychuk

Department of Veterinary Biosciences, College of Veterinary Medicine, The Ohio State University, Columbus, OH, USA

karniychuk.1@osu.edu

SUPPLEMENTAL MATERIALS AND METHODS

Cells

We maintained wild-type VERO E6 (VERO-ZAP-WT) and BHK-21 (BHK-ZAP-WT) cells, along with CCCH-type zinc finger antiviral protein (ZAP) knockout (ZAP-KO) derivatives (VERO-ZAP-KO and BHK-ZAP-KO), in DMEM (Fisher, MA, USA; #11-965-118) supplemented with 10% heat-inactivated fetal bovine serum (FBS, Fisher, MA, USA; #A5256801), 1x Penicillin-Streptomycin (Fisher, MA, USA; #15140122), and 2.67 mM sodium bicarbonate (Fisher, MA, USA; # 25080094) at +37°C in a 5% CO_2 humidified incubator.

To generate the VERO-ZAP-KO cell line, we previously used the guide RNA (gRNA) GTCTCTGGCAGTACTTGCGA targeting the first exon of the *Chlorocebus sabaeus* (Gene ID: 103226990) ZC3HAV1 gene, necessary for expressing all ZAP isoforms. A non-targeting gRNA (ACGGAGGCTAAGCGTCGCAA) served as the control [1,2]. These gRNAs were transiently transfected into cells using GenCrispr NLS-Cas9-NLS Nuclease (GenScript). Transfected cells were then seeded in 96-well plates through limiting dilution to generate isogenic single clones. After expansion, the clones were genotyped via Sanger sequencing using primers ATCGCTGGGCTGGACTAACG and GCAGAGAAGGGAGTGGCTGAA to identify location of indels on *Chlorocebus sabaeus* genome: -2 bp deletion, NW_023666072.1: 4677550-4677551). The knockout subclone confirmed by genotyping was further validated by western blot for ZAP expression in our previous studies [1,2]. Negative control cells were not isolated into single clones but were validated by Sanger sequencing to confirm the absence of indels. The same strategy was used to generate BHK-ZAP-KO cells with gRNA GGAGATCGTAGGCCAGACCGGGG targeting the first exon of the *Mesocricetus auratus*

(Gene ID: 110343172) Zc3hav1 gene and the same non-targeting control gRNA. After expansion, the clones were genotyped via Sanger sequencing with primers GCTGCTTCATCACCAAGATCC and GGTCGGGAAGACCCTTTCAC to identify location of indels on *Mesocricetus auratus* genome: -29 bp deletion, NW_024429200.1: 3564916-3564944). We confirmed the absence of mycoplasma contamination in all cells using the LookOut Mycoplasma PCR Detection Kit (Millipore Sigma, MA, USA; #MP0035).

In silico **permutation of the viral genome**

Certain experiments involving viral genomic mutations need permuted or scrambled virus control variants. Permutation can potentially impact the efficiency of reverse genetics methods. To simulate this scenario for ISA, we generated a permuted control for WNV. For permutation of WNV sequences we selected genomic regions encoding E and NS1 because these proteins are important for flavivirus pathogenesis, modulation of the infection cycle, viral RNA replication, and host immune evasion [27–29]. Moreover, we previously permuted these genomic regions in the Zika virus genome; this permutation did not affect Zika infection phenotypes *in vitro* and in mice [3]. We used an SSE 1.3 software package [30], specifically the CDLR randomizing in the SSE 1.3 [4-7]. During randomization we sought to avoid areas of the genome containing RNA elements that are required for replication or translation of the virus genome, such as cis-replicating elements, gene start or gene-end signals; we also avoided regions with prominent secondary structures. The CDLR randomizes the order of codons within the sequence while maintaining encoded proteins, dinucleotide frequencies, and coding parameters (**Table S2**).

70 **Infectious-Subgenomic-Amplicons (ISA) and virus stock generation**

71 The following reference sequences were used for *de novo* synthesis of flaviviruses: DENV type 2
72 strain 16681 [GenBank: U87411.1], JEV strain SA14-14-2 [GenBank: MK585066.1], and WNV
73 strain NY99 [GenBank: DQ211652.1]. To rescue DENV, JEV, and WNV, initially, we used
74 three overlapping (70-80 nt overlap) ISA DNA fragments (3,371-4,550 bp length) covering the
75 entire viral genome (**Table S1**; **File S1**); three overlapping DNA fragments is common ISA
76 strategy for flaviviruses [8,9]; thus, we consider it as a classical approach. The first and last
77 fragments for each virus are flanked with pCMV promoter and HDR/SV40pA sequences (**File**
78 **S1**).

79

80 Initially all DNA fragments for ISA were ordered through GeneScript (NJ, USA) or Twist
81 Biosciences (CA, USA) *synthetic clonal genes* services where DNA fragments are synthesized,
82 inserted into the bacterial plasmids (**Table S1**), amplified in bacteria, extracted, sequenced, and
83 plasmids with inserted fragments are delivered as lyophilized DNA with known concentration.
84 Some flavivirus ISA DNA fragments were toxic to bacteria, in both medium copy and low copy
85 plasmids (**Table S1**), and after multiple attempts *synthetic clonal genes* approach failed (see
86 results for details). To overcome this flavivirus DNA sequence toxicity to bacteria, we split toxic
87 clonal genes into two-four smaller overlapping fragments below 1.8 kb length. These smaller
88 size fragments allowed *synthesis of DNA* services from Twist Biosciences were DNA fragments,
89 flanked with 22 bp adapters (**File S1**), are rapidly (4-7 days service) synthesized without using
90 bacterial plasmids and bacteria. Twist Biosciences and GeneScript confirmed the correct
91 sequences of DNA fragments by next-generation-sequencing (NGS).

92

93 Overlapping clonal genes or synthetic DNA ISA fragments were amplified with high fidelity
94 Invitrogen Platinum PCR SuperMix High Fidelity (Fisher, MA, USA; #12-532-016) (primers are
95 in **Table S1**), mixed in equimolar concentration to obtain the final 1µg of DNA for transfection,
96 and transfected into BHK-ZAP-KO cell monolayers (6-well plates, five transfection replicates,
97 one mock-transfection control well) with Lipofectamine 3000 (Fisher, MA, USA; #L3000015) in
98 640 µl of OptiMEM (Fisher, MA, USA; #11-058-021)for 12 h at +37°C, 5% CO_2. Afterward,
99 OptiMEM media was removed and replaced with 3 ml of DMEM with 10% of FBS containing
100 $4x10^5$ VERO-ZAP-KO cells on the top of BHK-ZAP-KO cells and incubated plates for
101 additional 6-7 days (passage 0). For passage 1, 400 µl of media from each well of passage 0 was
102 transferred to wells with VERO-ZAP-KO cells and incubated for 4-7 days. During passages 0
103 and 1, cells were monitored for cytopathic effect (CPE). Generated flaviviruses were additionally
104 passaged 2-3 times on VERO-ZAP-KO cells to generate virus stocks; flasks were monitored for
105 CPE. Cell culture media from the final stocks were centrifuged (12,000 g, 20 min, +4°C),
106 aliquoted, and frozen (-80°C). Viral titers were quantified in duplicate in VERO-ZAP-WT and
107 VERO-ZAP-KO cells with endpoint dilution assay described below. The absence of mycoplasma
108 contamination in all virus stocks and cell cultures was confirmed using PCR Detection Kit
109 (Millipore Sigma, MA, USA; #MP0035).
110
111 To validate virus stock sequences, RNA was extracted from virus stock culture supernatants as
112 described below. PCR was performed using SuperScript™ IV One-Step RT-PCR System (Fisher,
113 MA, USA; #12-594-025) as per manufacturer's instructions with the primers targeting sequences
114 encoding E protein: DENV (Forward 5- GAC AGC TGT CAC TCC TTC AAT GAC-3 and
115 Reverse 5- CAT GCT CTT CCC CTG AGT GAG G-3); JEV (Forward 5-

116 GTTTTAATTGTCTGGGAATGGGC-3 and Reverse 5-GCCAACTTTGTATTTGATGTTTTC-
117 3); WNV-WT (Forward 5-CTATTGCTTTTGGTGGCCCCAG-3 and Reverse 5-
118 GTAGTTGGTCCATGGACAAA-3); WNV-Per (Forward 5-
119 CTATTGCTTTTGGTGGCCCCAG-3 and Reverse 5-GTAGTTGGTCCATGGACAAA-3). PCR
120 products were run on a 1% agarose gel, and DNA was purified and concentrated using DNA
121 Clean & Concentrator-5 (Zymo Research, CA, USA; # D4013) as per manufacturer's
122 instructions. DNA was sequenced by Sanger sequencing and sequences were aligned with
123 corresponding ISA sequences (**File S1**). Sanger sequencing confirmed correct sequences in
124 DENV, JEV, and WNV stocks.

125

126 **Comparative ISA**

127 To compare ISA efficiency on ZAP-WT and ZAP-KO cells, JEV and WNV fragments were
128 transfected into BHK+VERO-ZAP-WT or BHK+VERO-ZAP-KO cells as above. These
129 experiments were conducted simultaneously; also, the DNA amplicons for transfection in ZAP-
130 WT or ZAP-KO cells were obtained from the same PCR reactions. During passage 0, ZAP-WT
131 and ZAP-KO cells were observed for 5 (JEV) and 4 (WNV) days to compare CPE; the time was
132 shorter for WNV because it causes more aggressive infection and CPE. During the 1st passage,
133 CPE was observed, supernatants were collected on days 2-4 (2 for WNV; 4 for JEV) from each
134 well (5 replicates), RNA was extracted, and viral RNA loads were quantified with virus-specific
135 RT-qPCR. The shorter passage duration in the comparative ISA than in the initial ISA used for
136 virus rescue were applied to preserve cell monolayers for quantitative immunohistochemistry
137 (IHC) described below. The quantitative difference between ZAP-WT and ZAP-KO conditions
138 was represented by viral RNA loads in cell culture supernatants from five replicates.

139 Additionally, cellular monolayers from each transfected and mock-transfected well were fixed
140 and stained for viral E protein via IHC as described in the infectious virus titration below. To
141 quantify and compare IHC staining between ZAP-WT and ZAP-KO conditions, three images
142 (magnification x200) were randomly acquired in all five well replicates with the same
143 microscopic settings. Afterward, each image was processed in ImageJ (NIH)
144 (https://imagej.net/imaging/particle-analysis) with Automatic Particle counting [2].
145

146 **Animal experiments**

147 The animal studies were approved by The Ohio State University Institutional Biosafety
148 Committee (e-Protocol # 2022R00000111) and IACUC (e-Protocol #2023A00000095). Mice
149 were euthanized by deeply anesthetizing them with isoflurane, followed by cervical dislocation.
150

151 We conducted mouse experiments to identify whether ISA-rescued synthetic JEV and WNV
152 cause expected infection phenotypes which were previously described in mice infected with wild
153 or field isolates. The wild SA14-14-2 JEV strain does not cause clinical signs in conventional
154 mice; thus, we used *Ifnar1*$^{-/-}$ mice (The Jackson Laboratory, USA; Strain #:028288). The SA14-
155 14-2 JEV strain causes clinical signs or lethality in infected *Ifnar1*$^{-/-}$ mice [10]. After one week of
156 acclimatization, five-week-old mice (6 mice per group) were injected subcutaneously with the
157 virus-free media (MOCK) or 10^7 $TCID_{50}$/mouse of the ISA-derived SA14-14-2 JEV (**Table S1**).
158 Afterward, mice were monitored for clinical signs and body weight. Mice were sacrificed when
159 exhibiting greater than 20% weight loss or severe clinical signs. We sampled spleen and brain
160 from deceased mice, or from survived mice at the end of the study to quantify JEV loads.
161

162 The wild NY99 WNV strain causes severe infection in conventional C57BL/6J mice; thus, we
163 used the well-characterized C57BL/6J mouse lethal model [11-13]. Five-week-old C57BL/6J
164 mice (Strain #:000664; 14 mice per group) were ordered from The Jackson Laboratory,
165 acclimatized for a week, and injected intraperitoneally (IP) with the virus-free media (MOCK),
166 ISA-derived WNV wild-type (**Table S1**), or ISA-derived WNV permuted (WNV-Per) variant
167 (**Table S1**). For comparative purposes, we standardized mouse injection doses by normalization
168 of viral RNA loads (determined by RT-qPCR, see below) in the WNV-WT and WNV-Per
169 inoculums which resulted in 10^7 RNA copies/mouse for both variants (WNV-WT -
170 10^5 $TCID_{50}$/mouse; WNV-Permuted - $10^{5.6}$ $TCID_{50}$/mouse; titers quantified on VERO-ZAP-WT
171 cells, see below). Afterward, mice were monitored for clinical signs and body weight changes.
172 Mice were sacrificed when exhibiting 20% or greater weight loss or severe clinical signs, or at
173 the end of the study to sample spleen and brain from mice.
174

175 **Infectious virus titration**

176 To quantify infectious loads in DENV, JEV and WNV stocks, the endpoint dilution assay was used
177 to determine the 50% tissue culture infectious dose ($TCID_{50}$), with two replicates, as we had
178 described before [3,14-18]. Viral stocks were serially diluted in four replicates in media and 50 µl
179 of each dilution was added to confluent VERO-ZAP-WT or VERO-ZAP-KO cells cultured in 96-
180 well plates. Dilutions were made in DMEM media with 1% FBS. After 2 h at 37°C, 150 µl of
181 media was added. The cells were incubated for 5-7 days (5 days for WNV; 7 days for DENV and
182 JEV) at 37°C, 5% CO_2. Afterward, plates were washed, dried, formalin fixed, and stained with
183 specific antibodies (Ab) [3,14-18]. For DENV and WNV IHC, we used primary anti-pan flavivirus
184 envelop (E) protein monoclonal Ab D1-4G2-4-15 (ATCC, VA, USA; #HB-112) followed by Goat

185 anti-Mouse IgG HRP Ab (Abcam, MA, USA; #ab97023). For JEV, we used JEV E polyclonal Ab
186 (GeneTex, CA, USA; #GTX125867;) followed by Goat Anti-Rabbit IgG H&L (HRP) Ab (Abcam,
187 MA, USA; #ab97051) [3,14-18]. Infectious titers were calculated by the Spearman-Kärber formula
188 and expressed in $\log_{10}$ $TCID_{50}$ per ml. Media from mock-inoculated cells were used as negative
189 controls.
190

191 **RNA extraction and virus-specific reverse transcriptase quantitative polymerase chain**
192 **reaction assays (RT-qPCR)**

193 The RNA from cell culture supernatants was extracted with QIAamp Viral RNA Mini Kit
194 (QIAGEN) according to the manufacturer's instructions. The RNA from mouse tissues was
195 extracted with PureLink RNA Mini Kit (Invitrogen) according to the manufacturer's instructions.
196 All RT-qPCR reactions were conducted on the QuantStudio 3 real-time PCR system (Applied
197 Biosystems) and analyzed using QuantStudio Design & Analysis Software v1.5.2.
198 For DENV (F: 5′-AAGGACTAGAGGTTAKAGGAGACCC-3′; R: 5′-
199 GGCGYTCTGTGCCTGGAWTGATG-3′; Probe: 56-JOEN/AA CAG CAT A/ZEN/T TGA CGC
200 TGG GAA AGA CC-3IABkFQ), JEV (F: 5′-GCCACCCAGGAGGTCCTT-3′; R: 5′-
201 CCCCAAAACCGCAGGAAT-3′; Probe: 56-FAM-CAAGAGGTG/ZEN/GACGGCC-
202 3IABkFQ), and WNV (F: 5′-AGTAGTTCGCCTGTGTGAGC-3′; R: 5′-
203 GCCCTCCTGGTTTCTTAGA-3′; Probe: FAM-
204 AATCCTCACAAACACTACTAAGTTTGTCA-TAMRA) we used the previously validated
205 probe-based one-step RT-qPCR assays [19,20]. The Luna Universal Probe One-Step RT-qPCR
206 Kit (NEB) reaction mixture (20 μL) consisted of 10 μL Luna Universal Probe One-Step Reaction
207 Mix, 1 μL Luna WarmStart RT Enzyme Mix, 1 μL (10 μM) of forward and reverse primers, 0.5

208 μL of the probe, 2.5 μL nuclease-free water and 4 μL of RNA template. The reverse transcription
209 and enzyme activation steps of 10 min at 55˚C and 1 min at 95˚C were followed by 40
210 amplification cycles (10 s at 95˚C and 30 s at 60˚C). A standard curve was used to quantify viral
211 RNA loads as we described [14].
212
213 PCR values were corrected for fluid volumes or tissue weights and upon logarithmical
214 transformation expressed as virus RNA genome copies per ml or g. Strict precautions were taken
215 to prevent PCR contamination. All master mix preparations were done in the dedicated PCR
216 cabinet. Aerosol-resistant filter pipette tips and disposable gloves were used. Kit reagent controls
217 were included in every RNA extraction and PCR run.
218
219 **Statistics**
220 We used GraphPad 9 PRISM for statistics. For the comparison of the viral RNA loads, infectious
221 titers, and quantitative IHC we used an unpaired t-test. P-value < 0.05 was considered statistically
222 significant.
223
224
225
226
227
228
229
230

231 **REFERENCES**

232 1. Nguyen Phuong Khanh Le, Ahmad Jawad Sabir, Ivan Trus, Uladzimir Karniychuk. Endogenous ZAP
233 is associated with altered global cellular gene expression during Zika virus infection. bioRxiv.
234 2024.
235 2. Ahmad Jawad Sabir, Prince Pal Singh, Uladzimir Karniychuk. Endogenous ZAP affects Zika virus
236 RNA interactome. bioRxiv. 2024.
237 3. Trus I, Udenze D, Berube N, et al. CpG-Recoding in Zika Virus Genome Causes Host-Age-
238 Dependent Attenuation of Infection With Protection Against Lethal Heterologous Challenge in
239 Mice. Front Immunol. 2019;10:3077.
240 4. Simmonds P. SSE: a nucleotide and amino acid sequence analysis platform. BMC research notes:
241 BioMed Central; 2012. p. 50.
242 5. Gaunt E, Wise HM, Zhang H, et al. Elevation of CpG frequencies in influenza A genome
243 attenuates pathogenicity but enhances host response to infection. eLife2016. p. e12735.
244 6. Atkinson NJ, Witteveldt J, Evans DJ, et al. The influence of CpG and UpA dinucleotide frequencies
245 on RNA virus replication and characterization of the innate cellular pathways underlying virus
246 attenuation and enhanced replication. Nucleic acids research2014. p. 4527-45.
247 7. Tulloch F, Atkinson NJ, Evans DJ, et al. RNA virus attenuation by codon pair deoptimisation is an
248 artefact of increases in CpG/UpA dinucleotide frequencies. eLife2014. p. 1-15.
249 8. Park CJ, Lee YA, Yoo SM, et al. Efficient reverse genetics approach involving infectious
250 subgenomic amplicon for engineering dengue virus. J Med Virol. 2023 Aug;95(8):e28978.
251 9. Aubry F, Nougairede A, Gould EA, et al. Flavivirus reverse genetic systems, construction
252 techniques and applications: a historical perspective. Antiviral Res. 2015 Feb;114:67-85.
253 10. Liu J, Jing W, Fang Y, et al. The Infection of the Japanese Encephalitis Virus SA14-14-2 Strain
254 Induces Lethal Peripheral Inflammatory Responses in IFNAR Deficiency Mice. Frontiers in
255 microbiology: Front Microbiol; 2022.
256 11. Zhang YN, Li N, Zhang QY, et al. Rational design of West Nile virus vaccine through large
257 replacement of 3' UTR with internal poly(A). EMBO Mol Med. 2021 Sep 7;13(9):e14108.
258 12. Daffis S, Samuel MA, Keller BC, et al. Cell-specific IRF-3 responses protect against West Nile virus
259 infection by interferon-dependent and -independent mechanisms. PLoS Pathog. 2007 Jul
260 27;3(7):e106.
261 13. Daffis S, Samuel MA, Suthar MS, et al. Interferon regulatory factor IRF-7 induces the antiviral
262 alpha interferon response and protects against lethal West Nile virus infection. J Virol. 2008
263 Sep;82(17):8465-75.
264 14. Chapagain S, Pal Singh P, Le K, et al. Japanese encephalitis virus persists in the human
265 reproductive epithelium and porcine reproductive tissues. PLoS Negl Trop Dis. 2022
266 Jul;16(7):e0010656.
267 15. Sabir AJ, Singh PP, Trus I, et al. Asian Zika virus can acquire generic African-lineage mutations
268 during in utero infection. Emerg Microbes Infect. 2023 Dec;12(2):2263592.
269 16. Darbellay J, Lai K, Babiuk S, et al. Neonatal pigs are susceptible to experimental Zika virus
270 infection. Emerg Microbes Infect. 2017 Feb 15;6(2):e6.
271 17. Darbellay J, Cox B, Lai K, et al. Zika Virus Causes Persistent Infection in Porcine Conceptuses and
272 may Impair Health in Offspring. EBioMedicine. 25:73-86.2017.
273 18. Trus I, Udenze D, Cox B, et al. Subclinical in utero Zika virus infection is associated with interferon
274 alpha sequelae and sex-specific molecular brain pathology in asymptomatic porcine offspring. In:
275 Pierson TC, editor. PLoS Pathogens2019. p. e1008038.
276 19. Eiden M, Vina-Rodriguez A, Hoffmann B, et al. Two new real-time quantitative reverse
277 transcription polymerase chain reaction assays with unique target sites for the specific and

278 sensitive detection of lineages 1 and 2 West Nile virus strains. J Vet Diagn Invest. 2010
279 Sep;22(5):748-53.
280 20. Shao N, Li F, Nie K, et al. TaqMan Real-time RT-PCR Assay for Detecting and Differentiating
281 Japanese Encephalitis Virus. Biomedical and environmental sciences : BES: Biomed Environ Sci;
282 2018. p. 208-214.